



Journal of Materials and Engineering Structures

Research Paper

Comparison between DRF for displacement and acceleration spectra with uncertain damping for EC8

Baizid Benahmed ^{a,*}, Abbas Moustafa ^b, Mohamed Badaoui ^a

^a Development Laboratory in Mechanics and Materials, University of Djelfa, Algeria

^b Department of Civil Engineering, Faculty of Engineering, Minia University, Minia, Egypt

ARTICLE INFO

Article history:

Received : 31 May 2018

Revised : 15 January 2019

Accepted : 1 February 2019

Keywords:

Uncertainties

Damping reduction factor

Monte Carlo Simulation

High damping response spectra

ABSTRACT

The damping force exerted by a structure during an earthquake differs significantly from that specified in the design process. This introduces uncertainties in the design process of structures under earthquake loads. Accordingly, it is desirable to consider not only the effect of randomness of the seismic load but also the uncertainties in the structural parameters. This paper investigates the effect of uncertainties inherent in the damping ratio on the use of damping reduction factor (DRF) for the evaluation of high damping response spectra for linear structures with viscous damping. The DRFs are evaluated from both acceleration and displacement response spectra. Effects of period of vibration, level of damping ratio, soil class and uncertainties level of damping on the DRFs are evaluated and discussed. A numerical analysis implies that the maximum relative error estimated between the deterministic DRF and the DRF considering uncertainties in damping is about 14%. This implies that the damping uncertainty with $C_v\zeta = 20\%$ leads to an error in DRF of $C_v=13\%$ which is a significant error in estimating the structure response.

1 Introduction

Strong ground motion remains the first natural disaster causing massive damage of engineering structures and large lives losses worldwide [1]. Earthquake risk reduction includes avoiding construction near seismically active regions and seismic-resistant design of nuclear-power plants, infrastructures, industrial installations and buildings[2]–[4]. Earthquake-resistant design is generally based on designing a light weight structure, strong column-weak beam concept and minimizing the oscillations transmitted to the structure [2]–[4]. New technologies and modern techniques, such as active and passive structural control and structural-health monitoring have been employed in recent years to minimize the severe effect of strong ground motion on important structures, such as large-span bridges and skyscrapers[5], [6]. Active control of structures consists of installing sensors that are connected to a computer unite performing continuous analysis and monitoring of

* Corresponding author. Tel.: +213 671888201.

E-mail address: benahmed.tp@univ-djelfa.dz

structural response data followed by the application of certain force opposite to the dynamic force resulting from earthquakes or wind. On the other hand, passive structural control contains base-isolation of structures and installation of dampers to dissipate the dynamic force transmitted from the strong-ground motion to the structure. As is well known, the estimation of the structural response to dynamic loads depends on two factors, namely, the uncertainties involved in earthquake ground motion and the variability of the structures parameters. Earthquake uncertainties include randomness involved in ground motion energy, total duration, frequency-content, peak ground acceleration, etc. Variability of material properties includes stiffness, natural frequencies, Young's modulus, damping model and damping coefficient [7]. To reliably estimate the realistic seismic response of structures, it is essential to accurately quantify the effect of both the stochastic nature of the ground motion and the uncertainties associated with the dynamic properties of the structure (e.g., damping coefficient and natural periods) on their responses.

The structure uncertainties are mainly involved with the variation of the material properties and the approximations in the mathematical model utilized in the modelling process of the structure input-output dynamic problem. The inaccurate modelling of appropriate structural properties may introduce significant errors in estimating the structural response. Accordingly, it is often desirable to consider the effect of material variability in the analysis and design of dynamic problems [7], [8]. In this study, attention is given to the effect of the random nature of the damping coefficient on the seismic response of structures. Haviland [9] has shown that the Gamma and the lognormal distributions provide the best fit to the variations of the damping values with a coefficient of variation ($C_v\zeta$) in the range of 42-87% through an extensive analysis of the database. The study concluded that the $C_v\zeta$ ranges from 33 - 78 % and suggested an average value of 40 %.

Damping uncertainties are integrated in the process of the seismic response estimation in the evaluation of the damping reduction factor (DRF) that characterizes the adjusting of response spectra given in modern seismic codes for a damping ratio of 5 % at other damping levels [10]. The DRF has been studied by many researchers and different mathematical expressions have been proposed, as a function of the damping ratio [11]–[13], damping ratio and period [14]–[17], damping ratio, period and other earthquake characteristics (e.g. duration, soil conditions, epicentral distance, magnitude) [18]–[20]. The works cited above discussed the DRF derived from the displacement. The influence of seismological parameters (e.g., magnitude, epicentral distance and site condition) on DRF for acceleration spectra was analysed and discussed in [21], [22].

It may be noted that the DRF is mainly affected by the damping ratio, and thus the error in the damping estimation may lead to an incorrect estimation of the value of DRF causing inaccurate dynamic response estimation. This research work investigates the effect of uncertainties involved in estimation of the damping ratio ξ on the DRF value derived from the displacement and the acceleration responses. The commonly used viscous damping model is employed herein, and damping uncertainties are represented by a lognormal distribution function [9]. The Monte Carlo Simulation (MCS) technique is used to generate a large number of damping values. The most suitable number of samples (200 for each response spectrum) has been estimated using a statistical analysis.

Conclusions from numerical results that are important for structural engineers are obtained and their use can be extended to improve current seismic regulations of modern seismic codes.

2 Overview of damping reduction factors used on the literature

DRFs adopted in modern seismic codes are often derived from the effects of viscous damping on the displacement response of elastic single-degree-of-freedom (SDOF) systems as follows [16]:

$$DRF_d = \frac{SD(\zeta, T)}{SD(5\%, T)} = \frac{PSA(\zeta, T)}{PSA(5\%, T)} \quad (1)$$

Similarly, the values of DRF derived from the acceleration spectra are obtained as:

$$DRF_a = \frac{SA(\xi, T)}{SA(5\%, T)} \quad (2)$$

Where $SD(\zeta, T)$ and $SA(\zeta, T)$ are the spectral displacement and acceleration, respectively.

Several researchers have studied the DRF and different mathematical expressions have been proposed. One of the first formulation of the DRF is proposed by Newmark and Hall [23], in terms of three relationships holding respectively the

constant velocity, the constant acceleration and the constant displacement regions of the spectrum. Their results inspired many seismic codes and standards (e.g., ATC-40, FEMA-273 UBC-97, NEHRP-97)[24], [25]. The proposed expressions are expressed as[23]:

$$DRF = \begin{cases} 1.514 - 0.321 \ln(\zeta) & \text{for constant acceleration region} \\ 1.400 - 0.248 \ln(\zeta) & \text{for constant velocity region} \\ 1.309 - 0.194 \ln(\zeta) & \text{for constant displacement region} \end{cases} \quad (3)$$

The study carried out by Wu and Hanson [17] presented a set of DRF from a statistical study of inelastic response spectra with high damping ratios. They proposed the following expression of DRF:

$$DRF = \frac{\lambda(\zeta, T)}{\lambda(5\%, T)} \quad (4)$$

In which $\lambda(\zeta, T)$ is represented by a set of logarithmic relations.

The damping reduction factor proposed in Ref.[13]is expressed as:

$$DRF = \sqrt{\frac{0.05 \times (1 - e^{-\alpha \zeta})}{\zeta \times (1 - e^{-0.05 \alpha})}} \quad (5)$$

Where α is a coefficient ranging from 18 to 65 depending on the earthquake characteristics. These results were adopted in the UBC-94 and NEHRP-94 for the design of buildings with passive energy dissipation systems, given as:

$$DRF = \sqrt{\frac{10}{5 + \zeta}} \quad (6)$$

$$DRF = \sqrt{\frac{7}{2 + \zeta}} \quad (7)$$

Bommer and Elnashai [12] suggested a simple formula for the DRF, which was adopted in EC8 (2004) [10] (Eq.6).Their proposed expression replaced the earlier formula (Eq.7) of the pre-norm version of the code (EC8, 1994).

Lin and Chang (2003)[15]concluded that force reduction factors in seismic codes are force-based procedures, but the DRFs adopted by these codes are derived from the effects of viscous damping on the displacement response. According to their results, they concluded that this phenomenon will lead to unconservative estimation. They suggested that if the damping of a structure comes from the hysteretic behaviour (e.g., the plastic hinge), the DRFs should be derived from the acceleration response. Otherwise, if the additional damping of a structure comes from the added energy dissipation devices, the DRFs should be derived from the displacement response.

Lin et al. [26], [27] carried out a series of studies on DRF. These studies were focused on differentiating the damping effect on displacement and acceleration responses, and the effect of site condition on DRFs was investigated as well. Mathematical expressions are obtained from nonlinear regression analysis using the Levenberg–Marquardt method to estimate the DRF derived from the displacement and acceleration responses [16] as follows:

$$DRF = 1 - \frac{\alpha T^{0.80}}{(T + 1)^{0.65}} \quad (8)$$

Where

$$\alpha = 1.303 + 0.436 \ln(\zeta) \quad (9)$$

Benahmed et al. developed a new method to estimate the DRF using neural networks [28]. A procedure using Artificial Neural Network (ANN) was developed to compute DRF without recourse to mathematical formulation. The ANN was shown to provide accurate numerical results compared to the exact results and those given by the formulation of Lin [27]. Ref. [29] used this method to estimate the DRF for the EC8. The maximum relative error between the exact results and the ANN results

is about 10 % and reaching 25% for the formulation of EC8 for $T < 5$ s. The results obtained show that the use of ANN gives accurate results compared to EC8 formulation. The developed ANN can be used to estimate the DRF for different seismic codes with appropriate level of accuracy.

Recently, Palermo et al.[30]presented an analytical formulations of the DRF based on power spectral density functions. The surface ground motion is modelled with the Kanai–Tajimi power spectral density function (i.e. as an ideal white noise at the bedrock filtered through the soil deposit). Finally, Ref. [30]proposed a simple code-like formula:

$$DRF = \left(\frac{10}{5 + \zeta} \right)^\chi \quad (10)$$

The DRF proposed curves for 13 values of χ from 0.20 to 0.80 are provided in Ref.[30].

The effect of uncertainties in the estimation of damping ratio on DRF values for the evaluation of high damping response spectra are examined in [14]. Damping uncertainties are described by a lognormal probability distribution. Based on the results of this study, a new simple DRF formulation, accounting for uncertainties in damping estimation, is tentatively proposed, this formulation is applied only for $C_v \zeta = 20\%$ as follows:

$$DRF = 0.941 + \frac{0.009}{\zeta} + 0.028 \frac{\zeta}{T} - 1.335 \zeta \quad (11)$$

Benahmed [31]proposed a DRF formulation through a nonlinear regression for the Algerian Seismic Regulations (RPA 99 v 2003) (Eq.12), currently contain the old formula of EC8 (1994). The ground motions used in this study are selected from the world ground motion database PEER considering the soil classification of RPA.

$$DRF = 0.582 + 0.418 (12.279 - T)^{(-3.9(\zeta - 0.05))} \quad (12)$$

The proposed formulation accounts for the specificity of the Algerian code in terms of soil classification and the response spectrum of the RPA and gives accurate results for the estimation of DRFs. Accordingly, the above expression is recommended for the RPA in the estimation of the high-damping response spectrum.

3 Ground motion selection

The selection of seismic records is an essential step for many applications in structural dynamic analysis and design. Nowadays, trusted strong ground motion databases are available on the internet (e.g., Japanese earthquake strong-motion databases K-NET and KiK-net, PEER ground motion database –PGMD-, the Italian database, etc.). Structural engineers always have difficulties in record selection given the large number of recorded earthquake data on one hand and the scarce seismic data on the other hand. One of the tools used in this field is Rexel tool [32]. It allows searching for sets of records for a variety of structural applications which proved to provide an efficient selection in most cases [32].

Rexel is a tool that allows users to select sets of seismic records that are compatible with a pre-specified response design spectrum defined by the user. Herein, the user specifies a target response spectrum and the desired characteristics of the seismic records in terms of magnitude, epicentral distance, shear wave velocity V_{s30} and other general characteristics. Ground motions records are selected from the internal database that satisfy the user-specified selection criteria which provide best fit to the target response spectrum.

Similar to other modern seismic codes, Eurocode 8 (EC8) allows the use of natural earthquake records for the seismic analysis and design of structures. The main condition to be satisfied is that the average elastic spectrum does not underestimate the code spectrum by more than 10% tolerance, in a broad range of periods, depending on the structure's dynamic properties. However, in Sec. 4.3.3.4.3, the code allows the consideration of the mean effects on the structure, rather than the maximum (should a minimum of three accelerograms be used), if at least seven nonlinear time- history analyses are performed.

In this study the Rexel tool has been used to select three sets of seven natural records which are closer possible as average to the EC8 design spectra with 475 years return period ($PGA_{ag} = 0.35$ on stiff soil). The list of all the records selected for each soil class, with their main characteristics, is listed in the Tables 1-3. According to EC8, soil type A corresponds to rock,

soil type B represents deposits of very dense sand, gravel, or very stiff clay and soil type C is deep deposits of dense or medium-dense sand, gravel or clay.

In Figure 1-3, the EC8 target spectrum is compared to the average response spectrum derived from the seismic records for the three soils.

Table 1 - Response spectra of the records returned by REXEL for soil type A

Earthquake Name	Station ID	Date	Mw	Fault Mechanism	Epicentral Distance (km)
Tabas	ST54	1995_10_01	7.3	oblique	12
Friuli	ST20	1976_05_06	6.5	thrust	23
Bingol	ST539	2003_05_01	6.3	strike slip	14
South Iceland	ST2486	2000_06_17	6.5	strike slip	5
Tabas	ST54	1978_09_16	7.3	oblique	12
Friuli	ST20	1976_05_06	6.5	thrust	23
South Iceland (aftershock)	ST2558	2000_06_17	6.4	strike slip	5

Table 2 - Response spectra of the records returned by REXEL for soil type B

Earthquake Name	Station ID	Date	Mw	Fault Mechanism	Epicentral Distance (km)
Erzincan	ST205	1995_10_01	6.6	strike slip	13
South Iceland	ST2482	2000_06_17	6.5	strike slip	15
Montenegro	ST67	2000_06_21	6.9	thrust	16
South Iceland	ST2484	2000_06_17	6.5	strike slip	7
Montenegro	ST62	1979_04_15	6.9	thrust	25
South Iceland (aftershock)	ST2488	2000_06_17	6.4	strike slip	11
Montenegro	ST67	1979_04_15	6.9	thrust	16

Table 3 - Response spectra of the records returned by REXEL for soil type C

Earthquake Name	Station ID	Date	Mw	Fault Mechanism	Epicentral Distance (km)
Dinar	AI_137_DIN	1995_10_01	6.4	normal	0.47
EMILIA_Pianura_Padana	MRN	2012_05_29	6.0	reverse	3.58
Dinar	AI_137_DIN	1995_10_01	6.4	normal	0.47
Erzincan	ERZ	1992_03_13	6.6	strike-slip	8.97
N Miyagi Prefecture	MYG010	2003_07_25	6.1	reverse	9.93
Mid Niigata Prefecture	NIG020	2004_10_23	6.3	reverse	8.99
Mid Niigata Prefecture	NIG019	2004_10_23	6.6	reverse	7.01

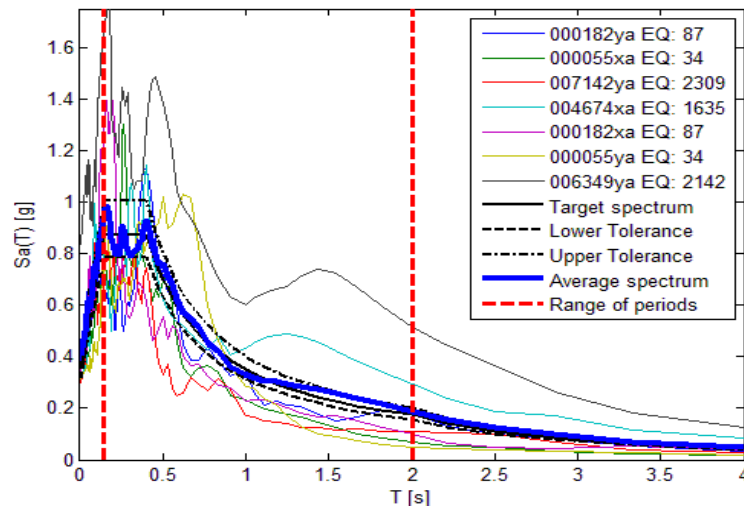


Fig. 1 - Response spectra of the records returned by REXEL for soil type A

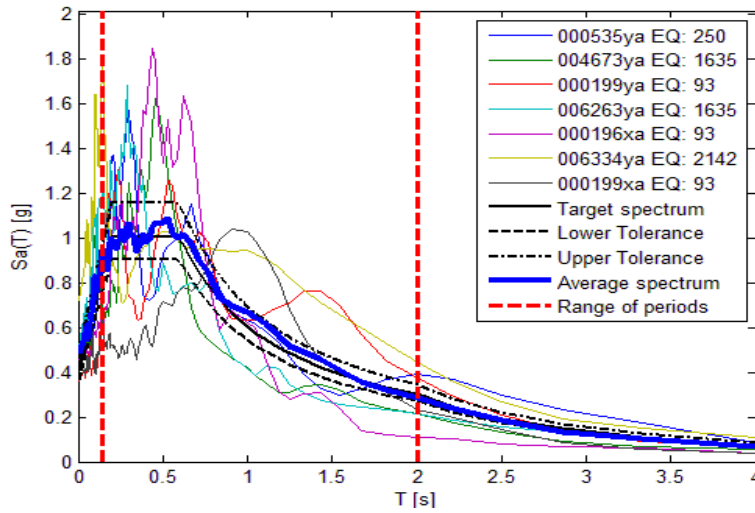


Fig. 2 - Response spectra of the records returned by REXEL for soil type B

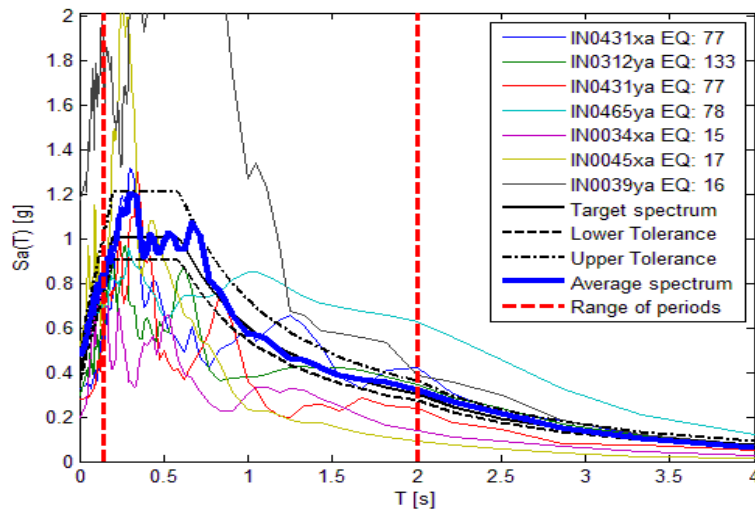


Fig. 3 - Response spectra of the records returned by REXEL for soil type C

4 Uncertainty in structural proprieties

The evaluation of the damping, resulting in part to the material of the structure is a controversial subject in practice. To identify this problem, several researchers have conducted tests at different levels of response amplitudes as well as for different types of structures and systems of different materials (e.g., concrete, steel and timber). Ref. [9] reported a wide range of data for different levels of response amplitudes and large classes of structural systems and sizes of buildings. This study has shown that Gamma and lognormal distributions provide the best fit to the variations of damping. The coefficient of variation ($C_{v\zeta}$) of damping estimates based on adopted data set varied in the range of 42-87%. Ref.[33]re-examined the database, noted that $C_{v\zeta}$ ranges from 33 to 78% and suggested a value of 40% [8].

The uncertainties in natural period of the structure are related to assumptions made in modelling the stiffness and masse of structural elements. For example, for some structures such as vehicle parking, for example, the mass on each level is a function of time (days, seasons, etc.) and it is virtually impossible to predict its exact value during a future earthquake. Additionally, if the structure is constructed on soft soil, the phenomenon of soil-structure interaction cannot be ignored. In fact, characteristics of the structure depend on the dynamic properties of the foundation-soil pair which may differ before, during, and after an earthquake. Kareem [8] reported that the coefficient of variation characterizes the period uncertainties is taken as 0.17.

Haviland [9] reported that the primary source of uncertainty is the lack of understanding of damping mechanisms, other sources of uncertainties arise from:

- Amount of damping provided by substructure.
- Effect of duration of motion on the time dependent change in damping.
- Effect of previous vibrational elements.
- Participation of non-structural elements.
- Percentage of critical damping of higher modes.
- Change in damping at various amplitude levels.

The Monte Carlo Simulation method is used to generate the distribution of the random values of damping ratio values using the lognormal probability distribution function. Based on this assumption, the random values of the sample DRF of size n (i.e., $i=1$ to n) of corresponding responses are also independent, identically distributed and moreover, by virtue of the law of large numbers, the characteristics of the random sample approach even more statistical characteristics of the population as the sample size n increases.

This approach may be viewed as a synthetic or computer-generated experiment in which a probabilistic problem is analysed numerically through a sampling experiment [8]. The simulation procedure can be described in the following steps:

- Define the problem in terms of all random variables.
- Quantify the probabilistic characteristics of all random variables.
- Generate a sequence of sample values of the random variables with the prescribed distribution,
- Assess the problem in a deterministic manner for each a sequence of sample of all random variables.
- Perform statistical analysis of numerical results.
- Determine the effectiveness and accuracy of the method.

5 Development method

The objective of this analysis is the estimation of DRF values, taking into account the inherent uncertainties in ξ . A database of the DRF values is calculated by the following steps:

1. Selection of seismic records compatible with the design spectra of EC8 using Rexel. Thus, for each soil type, a set of 7 seismic records compatible with the EC8 design spectrum is selected.
2. Selection of $k=4$ damping ratio values ($\zeta = 7.5\text{-}20\%$) each being considered as a target value around which will be generated, using the Monte Carlo method, the random values ζ_k^m ($m = 1$ to 200) compatible with the lognormal probability distribution describing the uncertainties inherent to damping. The optimal number $n = 200$ of values generated with the MCS method was obtained by performing the "sampling test". The generation around the target value was done considering 3 values of $C_v\zeta$ in the interval $[5, 10, 20\%]$ on the basis of empirical estimates [9].
3. Computing, for each class S_i ($i = 1$ to 3) of soil and for each pair of values (ζ_k, T_j) ($k = 1$ to 4 and $j = 1$ to 32), 1400 values of the DRF (200 random values of the damping for 7 real accelerograms). Note that, regardless of the soil class considered, the DRF values estimated for the target value $\zeta_1 = 5\%$, will be different from 1 since it is calculated by considering values $\zeta_1^m \neq 5\%$ randomly generated around ξ_1 .
4. Development of the database composed of DRF target values, denoted DRF_d derived from displacement response (DRF_a derived from acceleration response), taking into account the effect of the uncertainties on ξ . For each pair of values (ζ_k, T_j), the target value $DRF_d^{S_i}(\zeta_k, T_j)$ are estimated using the following equation:

$$DRF_d^{S_i}(\zeta_k, T_j) = \mu_{DRF}^{S_i}(\zeta_k, T_j) + \sigma_{DRF}^{S_i}(\zeta_k, T_j) \tag{13}$$

where $\mu_{DRF}^{S_i}(\zeta_k, T_j)$ represents, for each pair of values (ζ_k, T_j) , the average of the 10000 estimated values of the DRF formulated as follows for each site S_i :

$$\mu_{DRF}^{S_i}(\zeta_k, T_j) = \frac{1}{1400} \sum_{l=1}^7 \sum_{m=1}^{200} DRF_{d,l}^{S_i}(\zeta_k, T_j) \tag{14}$$

Where l and m are the indices respectively associated with the l th seismic record considered among 7 records selected for the soil class S_i considered and at the same value ζ_k^m of the damping ratio among the 200 values generated around the target value ζ_k ($k = 1$ to 4) using MCS. The parameter $\sigma_{DRF}^{S_i}(\zeta_k, T_j)$ represents the standard deviation of the 1400 DRF values around ζ_k . For each pair of values (ζ_k, T_j) , the value $DRF_d^{S_i}(\zeta_k, T_j)$ expresses the effect of the soil class S_i ($i = 1$ to 3) on the DRF estimate. The values of $DRF_d^{S_i}(\zeta_k, T_j)$ are estimated for each value of $C_v\zeta$ (5, 10 and 20 %).

6 Numerical Results

6.1 Number of samples required

An estimate of the number of simulations required for a given physical problem constitutes a very important point of debate in the random computations. The Monte Carlo simulation is used to generate the values of DRF (ζ, T) associated to a structure with an uncertain damping ratio ζ . The values generated of the random variable ζ are independent, and in our case, following the Log-normal distribution.

Under this assumptions, the random values of the sample DRF (ζ, T) of size n ($i = 1, 2, \dots, N$) are also independent and moreover, by virtue of the law of large numbers, the characteristics of the random sample approach even more statistical characteristics of the population that the sample size N increases.

The aim here is to find the minimal number of simulations that gives representatives results with a minimum cost in term of time. The number of response spectra calculated for each value of ζ simulated is $7 \times 32 \times 4 \times 3$ where 7 is the number of records for each soil class, 32 is the number of periods, 4 is the number of ζ considered and 3 is the number of variation coefficients. Therefore, increasing the number of simulations from N to $N+1$ leads to multiplying the number of response spectrums to be calculated by 2688 times. This justifies the problem of increasing the number of simulations to a very high value of N .

For a given period T , the estimation of μ_{DRF} is established with a number of simulation N starting from to $N=5$ to $N=250$. The operation is repeated 100 times for each value of N and the results are presented in fig. 4.

If the values of μ_{DRF} becomes practically non-sensible to variation of N (if the operation is repeated with same number of simulation N) and that the standard deviation of the 100 values of μ_{DRF} tends to zero, the number N is sufficient to estimate reliably the values of DRF. Mathematically, this is expressed as:

$$\mu_{DRF}(\zeta_k, T) = \sum_{k=1}^N DRF(\zeta_k, T) \tag{15}$$

Figure 4 shows the results obtained for the values limits used in this study ($\zeta = 0.20$ and $C_v\zeta = 0.20$). This presents the maximum of perturbation of results around the mean values of ζ (if the number of simulation is sufficient automatically is sufficient for lesser values of ζ and lesser values of $C_v\zeta$).

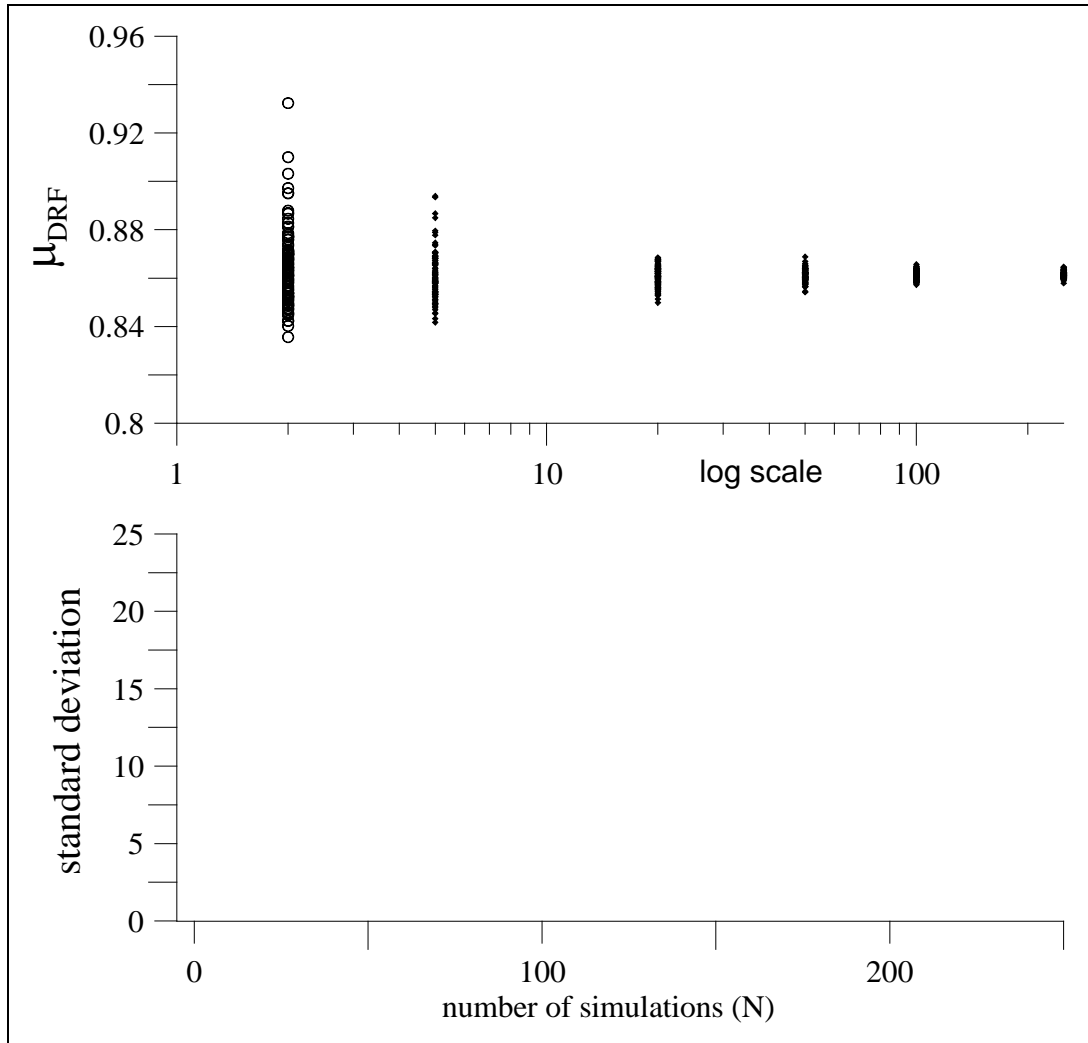


Fig. 4 – Sampling number

It is clear from the figure 4 that increasing the number of simulations from 5 to 200 have a significant influence on the perturbation of μ_{DRF} and that the standard deviation decreases when N increases. For $N=5$, the results average changes from $\mu=0.836$ to 0.932 and its standard deviation is equal to 0.01 . The relative error between the values of μ reaches 11.48% . For $N=200$, the results average changes from $\mu_{DRF}=0.857$ to 0.864 and its standard deviation is equal to 0.001 . The relative error between the values of μ_{DRF} is 0.8% . This implies that $N=200$ is a sufficient number of simulations for this case of study since it gives reliable results.

6.2 DRF obtained for displacement and acceleration spectra

Figure 5 depicts the ratio of DRF_d / DRF_{det} between DRF_d (DRFs derived from displacement response spectra considering inherent uncertainties to damping for $C_v\zeta = 5, 10$ and 20%), and the deterministic DRF values DRF_{det} (considering deterministic damping, i.e., uncertainty = 0).

The results are presented for soil types A, B, and C for damping ratios of $7.5, 10,$ and 20% , respectively. Figure 6 presents the results obtained for DRFs derived from the acceleration spectra.

It can be observed from figures 5 and 6 that the values obtained from earthquakes recorded for soil type A is slightly greater than that for other soil classes. The magnitude and trend of the curves are quite close regardless of the value of

damping ratios and the value of $C_v\zeta$ is somewhat independent of soil conditions. The values of DRF_d / DRF_{det} are slightly greater than that of DRF_a / DRF_{det} and the maximum values are 1.13 and 1.09 respectively. This implies that the DRF (DRF_d) derived from the displacement response are more sensitive to the uncertainties inherent to damping than the DRF (DRF_a) derived from the acceleration response. As can be expected, it is observed from figures 5 and 6 that the values of the DRF increases when $C_v\zeta$ increases. The relative error estimated between the deterministic values of DRF and DRF_d for each type of site reaches about 13%. Additionally, the maximum error obtained is about 11.79 % for soil type A, 10.08 % for soil type B and 13.33 % for soil type C.

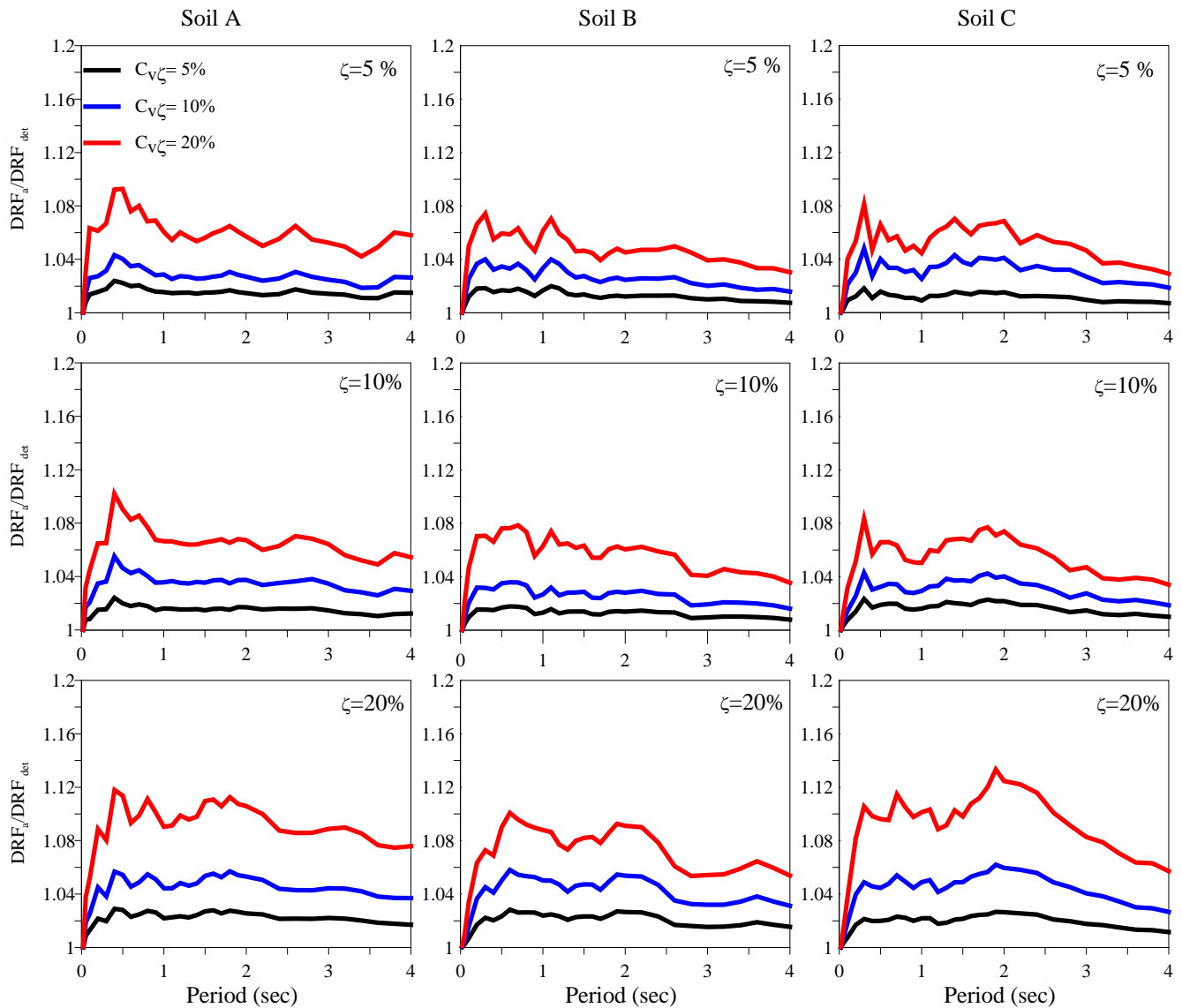


Fig. 5 – DRFs derived from displacement response.

The above results imply that the uncertainty in the estimation of damping values with $C_v\zeta = 20\%$ leads to an error on DRF_d with $C_v\zeta = 13\%$ which is a significant error that may put the structures on risk. The error between the deterministic values of DRF and DRF_a is around of 8.60% for soil class A and B, and 8.43% for soil class C. This confirms that the uncertainties in damping have more influence on DRFs derived from displacement than those derived from acceleration responses. The DRFs derived from displacement response are substantially different from those derived from the acceleration response. This should be taken into consideration before using these factors.

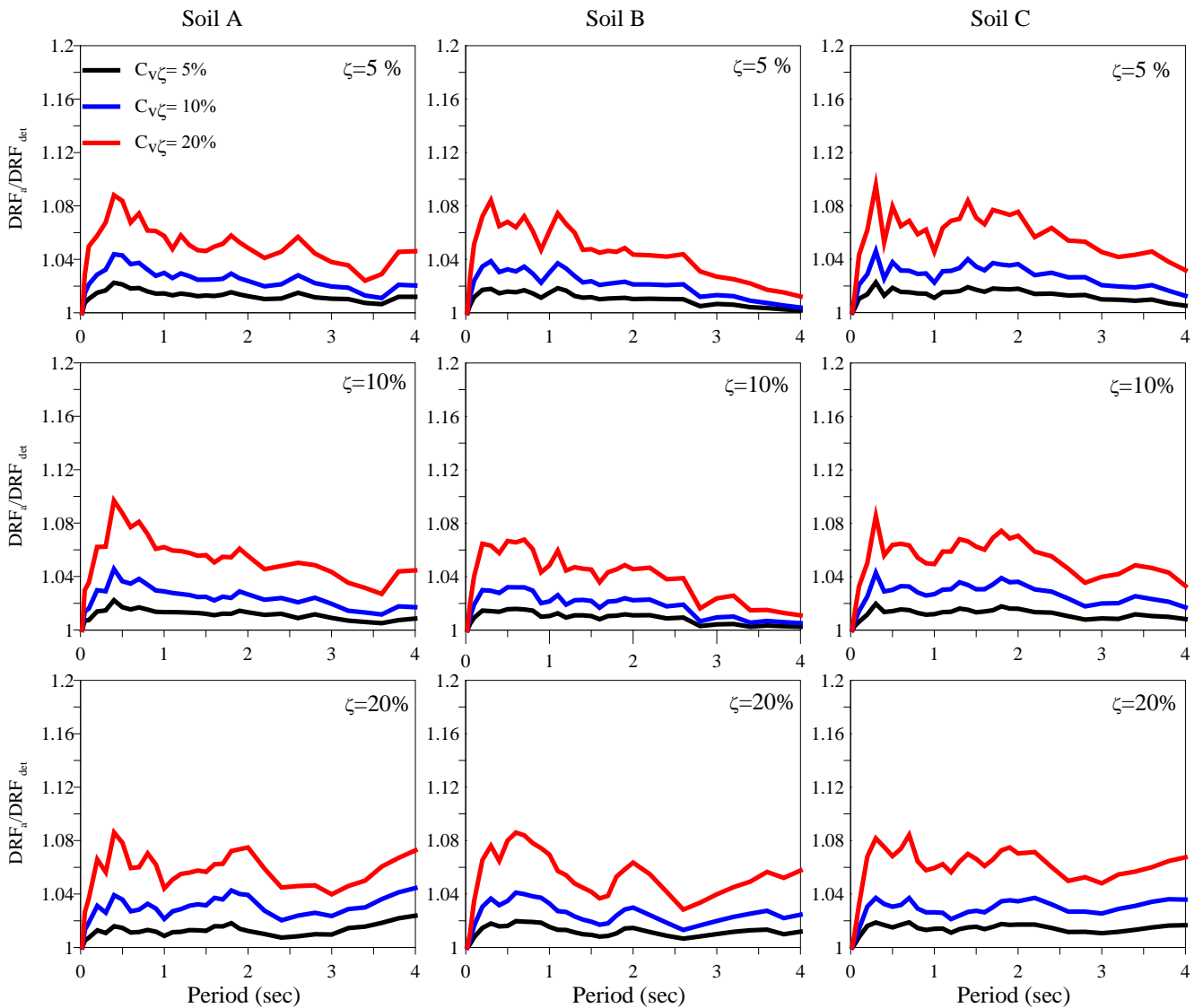


Fig. 6 - DRFs derived from acceleration response.

6.3 Discussion of soil effects

Site classification is always included in seismic design codes. The response spectra are significantly different from soil to another. Therefore, it is interesting to examine whether DRFs being used in design also depend on soils characteristics.

The soil type effect is estimated by comparing the values of $DRF^{S_i}(\xi_k, T_j)$ associated respectively with each of the three classes of soils S_i ($i = 1$ to 3), to their average value $DRF_{all}(\xi_k, T_j)$ given by:

$$DRF_{all}(\xi_k, T_j) = \frac{1}{3} \sum_{i=1}^3 DRF^{S_i}(\xi_k, T_j) \tag{16}$$

Which represent for each pair of values (ξ_k, T_j) a DRF value that neglects the site effect.

Figure 7 shows the DRF obtained for each soil normalized through average (DRF_{all}) for $C_v\zeta = 20\%$ and $\xi = 20\%$. A value of this ratio equal to unity means that the soil condition is completely negligible. As can be expected, it can be observed from this figure that the fluctuations of the representative curves for different classes oscillate around the value 1 and regardless the value of $C_v\zeta$ and ξ . It is clear from the figure that the influence of the soil type on DRFs increases while the damping

ratio increases. A relative error between DRF_{all} and DRF_d is estimated for each site for $C_{v\zeta} = 20\%$. For $\xi = 20\%$, the maximum error is 11.29 % for soil A, 7.32% for soil B and 6.75 % for soil C. The error between DRF_{all} and DRF_a (DRFs derived from acceleration response) is 11.15 for soil A, 8.07 % for soil B and 7.47 for soil C. Based on these results, it can be concluded that there is a weak dependence between the values of the DRF found and the type of soil.

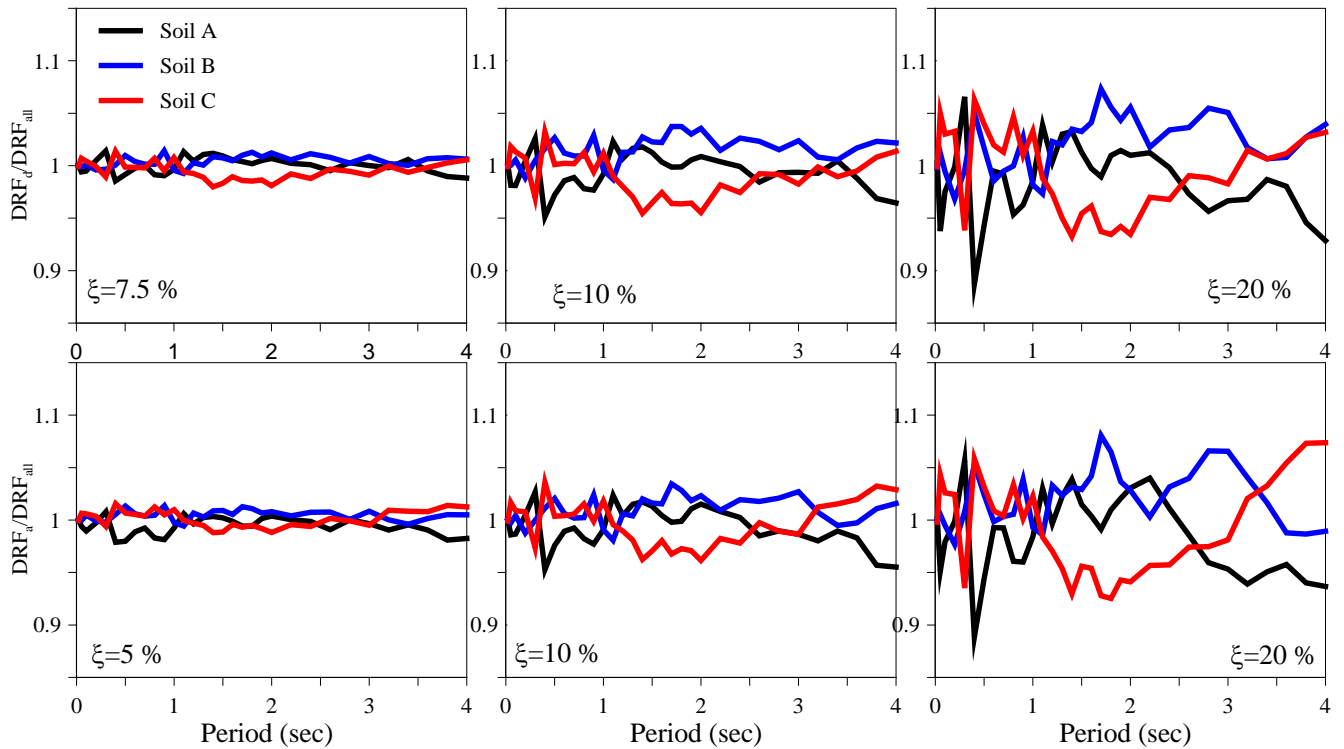


Fig. 7 - Soil effect

7 Concluding Remarks

In this paper, the effect of damping uncertainties on the damping reduction factor has been investigated for the DRF derived from displacement and acceleration response. A procedure to estimate the DRF including damping uncertainty was proposed. This method explicitly incorporates the uncertainties inherent in the damping of structures. A database containing DRF values associated with values $(T, \zeta, C_{v\zeta})$ has been developed based on three sets of seven natural earthquake records compatible with EC-8 spectra corresponding to three soil classes specified in EC-8.

The conclusions and suggestions drawn from this study can be summarized as follows:

An analysis of the effect of soil classes on the estimated DRF values implies that there is a low dependence between the values of the DRFs found and the type of soil.

It is observed from the numerical results obtained that the values of DRF considering damping uncertainty have magnitudes and trend of curves quite close regardless of damping ratios. Additionally, the values of $C_{v\zeta}$ are independent of soil class for both of both acceleration and displacement DRFs. The value of DRF increases when the damping uncertainty increases.

The ratio of DRFs derived from the displacement and the deterministic damping (DRF_d / DRF_{det}) is slightly greater than the respective value derived from acceleration and deterministic damping (i.e., DRF_a / DRF_{det}). The maximum values of these ratios are 1.13 and 1.09 respectively, indicating that the DRF (DRF_d) derived from the displacement response are more sensitive to the uncertainties inherent to damping than the DRF (DRF_a) derived from the acceleration response.

The relative error estimated between the deterministic values of DRF and DRFd for each type of site reaches about 14%. The maximum error obtained is around 11.79 % for soil A, 10.08 % for soil class B and 13.33 % for soil C. This implies that the uncertainty in the estimation of damping values with $C_v\zeta = 20$ % leads to an error in DRFd values with $C_v\zeta = 13$ % which is a significant error in estimating the structure response that may put the structures on risk.

REFERENCES

- [1]- D. Sanderson, A. Sharma. World Disasters Report 2016 - Resilience: Saving lives today, investing for tomorrow. The International Federation of Red Cross and Red Crescent Societies, 2016.
- [2]- D.J. Dowrick, Earthquake resistant design and risk reduction. Wiley, Second Edition, 2009.
- [3]- A. Moustafa, Earthquake-Resistant Structures - Design, Assessment and Rehabilitation. InTechOpen, 2012. doi:10.5772/2460
- [4]- I. Takewaki, A. Moustafa, K. Fujita, Improving the Earthquake Resilience of Buildings. Springer, 2013. doi:10.1007/978-1-4471-4144-0
- [5]- A. Seranaj, Dynamic Response and Seismic Analysis of Base Isolated Buildings: Monograph, Scholar's Press, 2016.
- [6]- A. Moustafa, S. Mahadevan, M. Daigle, G. Biswas, Structural and sensor damage identification using the bond graph approach. Struct. Control Heal. Monit. 17(2) (2010) 178–197. doi:10.1002/stc.285.
- [7]- A. Moustafa, S. Mahadevan, Reliability analysis of uncertain structures using earthquake response spectra. Earthquakes Struct. 2(3) (2011) 279–295. doi:10.12989/eas.2011.2.3.279
- [8]- A. Kareem, Aerodynamic response of structures with parametric uncertainties. Struct. Saf. 5(3) (1988) 205–225. doi:10.1016/0167-4730(88)90010-0
- [9]- R. W. Haviland, A study of the uncertainties in the fundamental translational periods and damping values for real buildings. Massachusetts Institute of Technology, 1976, pp. 115.
- [10]- Eurocode 8 (EC8). Design of structures for earthquake resistance, part 1: General rules, seismic actions and rules for buildings. 1988, pp. 219.
- [11]- S.V. Tolis, E. Faccioli, Displacement design spectra. J. Earthq. Eng. 3(1) (1999) 107-125. doi:10.1080/13632469909350342
- [12]- J. J. Bommer, A. S. Elnashai, Displacement Spectra for Seismic Design. J. Earthq. Eng. 3(1) (1999) 1–32. doi:10.1080/13632469909350338.
- [13]- S. Ashour, Elastic seismic response of buildings with supplemental damping, PhD Thesis, University of Michigan, 1987.
- [14]- B. Benahmed, M. Hammoutene, D. Cardone, Effects of damping uncertainties on damping reduction factors. Period. Polytech. Civ. Eng. 61(2) (2017) 341–350. doi:10.3311/PPci.9665
- [15]- Y. Y. Lin, K. C. Chang, Study on Damping Reduction Factor for Buildings under Earthquake Ground Motions. J. Struct. Eng. 129(2) (2003) 206–214. doi:10.1061/(ASCE)0733-9445(2003)129:2(206)
- [16]- Y. Y. Lin, K. C. Chang, Effects of site classes on damping reduction factors. J. Struct. Eng. 130(11) (2004) 1667–1675. doi:10.1061/(ASCE)0733-9445(2004)130:11(1667)
- [17]- J. Wu and R. D. Hanson, Study of Inelastic Spectra with High Damping. J. Struct. Eng. 115(6) (1989) 1412–1431. doi:10.1061/(ASCE)0733-9445(1989)115:6(1412)
- [18]- W. I. Cameron, R. A. Green, Damping correction factors for horizontal ground-motion response spectra, Bull. Seismol. Soc. Am. 97(3) (2007) 934–960. doi:org/10.1785/0120060034
- [19]- G. D. Hatzigeorgiou, G. A. Papagiannopoulos, Discussion on “Damping coefficients for near-fault ground motion response spectra”. Soil Dyn. Earthq. Eng. 31(4) (2011) 723–724. doi:10.1016/j.soildyn.2010.12.010
- [20]- R. Greco, A. Fiore, B. Briseghella, Influence of soil type on damping reduction factor: A stochastic analysis based on peak theory. Soil Dyn. Earthq. Eng. 104 (2018) 365–368. doi:10.1016/j.soildyn.2017.10.020
- [21]- H. Li, F. Chen, Damping modification factors for acceleration response spectra. Geod. Geodyn. 8(5) (2017) 361–370. doi:10.1016/j.geog.2017.04.009
- [22]- Y. Y. Lin, M. H. Tsai, K. C. Chang, On the Discussion of the Damping Reduction Factors in the Constant Acceleration Region for ATC-40 and FEMA-273. Earthq. Spectra. 19(4) (2003) 1001–1006. doi:10.1193/1.1623784
- [23]- N. Newmark, W. Hall, Earthquake Spectra and Design, Earthquake Engineering Research Institute (EERI) Monographs. 1982.
- [24]- ATC-40, Seismic evaluation and retrofit of concrete buildings. Applied Technology Council, 1996.

-
- [25]- Federal Emergency Management Agency (FEMA), NEHRP Recommended provisions for seismic regulations for new buildings and other structures. Council of the National Institute of Building Sciences, 2000.
- [26]- Y. Y. Lin, E. Miranda, K. C. Chang, Evaluation of damping reduction factors for estimating elastic response of structures with high damping. *Earthq. Eng. Struct. Dyn.* 34(11) (2005) 1427–1443. doi:10.1002/eqe.499
- [27]- Y. Y. Lin, Statistical study on damping modification factors adopted in Taiwan's seismic isolation design code by using the 21 September 1999 Chi-Chi earthquake. *Taiwan, Eng. Struct.* 29(5) (2007) 682–693. doi:10.1016/j.engstruct.2006.06.006
- [28]- B. Benahmed, M. Hamoutenne, B. Tiliouine, M. Badaoui, Prediction of the damping reduction factor by neural networks. *Asian J. Civ. Eng.* 17(2) (2016) 225-234.
- [29]- B. Benahmed, M. Hamoutenne, Use of the Artificial Neural Networks to Estimate the DRF for Eurocode 8. *Period. Polytech. Civ. Eng.* 62(2) (2018) 470-479. doi:10.3311/PPci.8139.
- [30]- M. Palermo, S. Silvestri, T. Trombetti, Stochastic-based damping reduction factors. *Soil Dyn. Earthq. Eng.* 80 (2016) 168–176. doi:10.1016/j.soildyn.2015.09.014
- [31]- B. Benahmed, Formulation of damping reduction factor for the Algerian seismic code. *Asian J. Civ. Eng.* 19(4) (2018) 375–385. doi:10.1007/s42107-018-0023-6.
- [32]- I. Iervolino, C. Galasso, E. Cosenza, REXEL: Computer aided record selection for code-based seismic structural analysis. *Bull. Earthq. Eng.* 8(2) (2010) 339–362. doi:10.1007/s10518-009-9146-1.
- [33]- A. G. Davenport, P. Hill-Carroll, Damping in Tall Buildings: Its Variability and Treatment in Design. In: *Proceedings of American Society of Civil Engineers (ASCE) Spring Convention, Seattle, ASCE, 1986, pp. 42–57*